Quantization of 5D Field Theories and New Regularization

Workshop "Development of Quantum Field Theory and String Theory" at YITP, Kyoto University
2008.7.28-8.1

S. Ichinose

August 1, 2008

Laboratory of Physics, School of Food and Nutritional Sciences, University of Shizuoka
Yada 52-1, Shizuoka 422-8526, Japan

ArXiv:0801.3064 flat
ArXiv:0808.???? warped

1. Introduction

Energy Spectrum of Radiation Filed

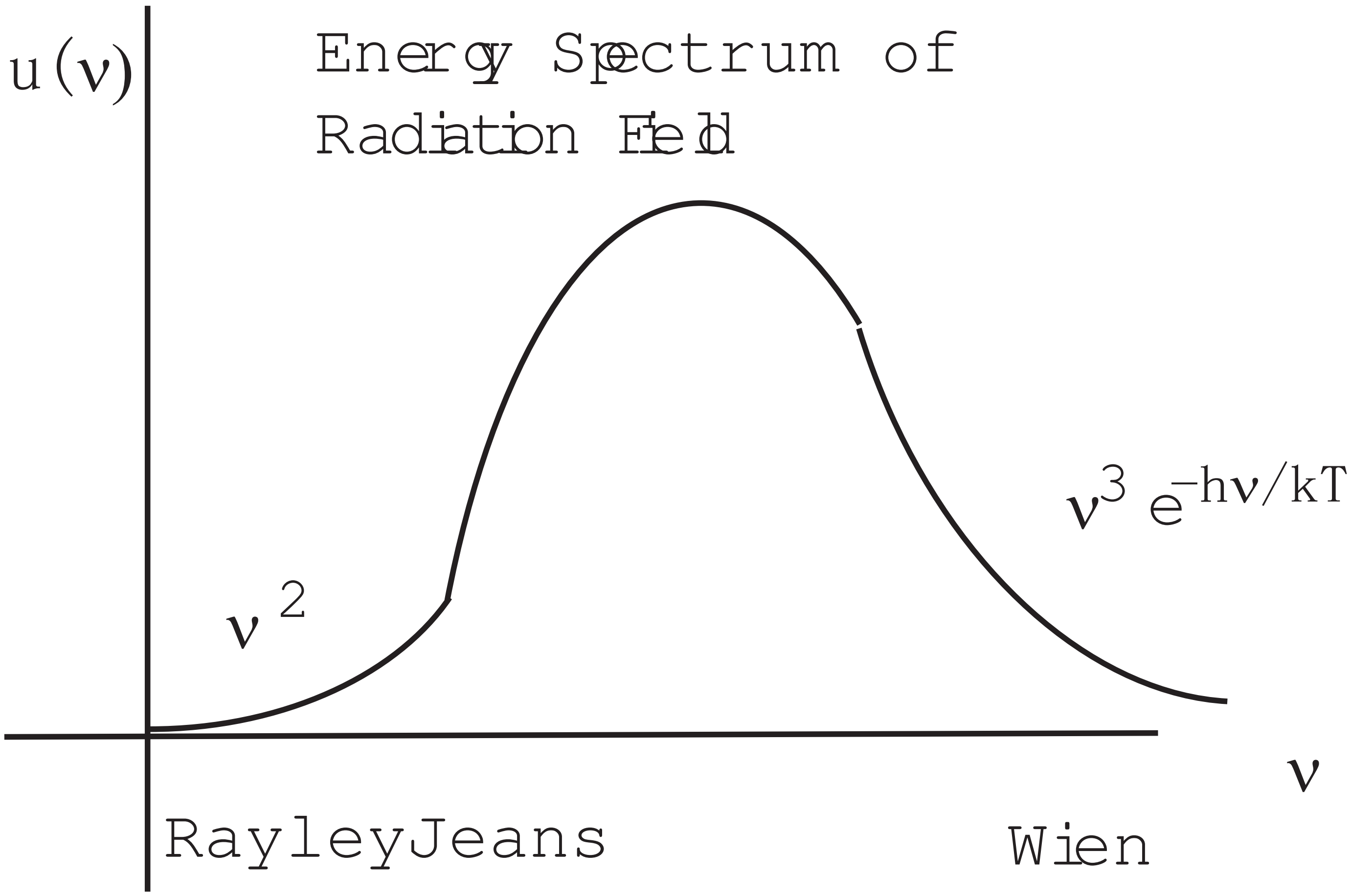

Rayley-Jeans formula $\longrightarrow$ Divergences of Specific Heat

Planck's formula $\dfrac{h\nu}{e^{\frac{h\nu}{kT}}-1} = h\nu\left(e^{-\frac{h\nu}{kT}} + e^{-\frac{2h\nu}{kT}} + e^{-\frac{3h\nu}{kT}} + \cdots\right)$

—— sum over all ν $\rightarrow$ Stephan's formula $U = 3\,\zeta(4) \times T^4$

$\dfrac{h\nu}{2}$ Zero-Point Energy $\longrightarrow$ Casimir Energy

Energy is discretized : $0,\ h\nu,\ 2h\nu, 3h\nu, \cdots$

1. 5D Quantum Electromagnetism

Flat Case

$$ds^2 = \eta_{\mu\nu}dx^\mu dx^\nu + dy^2 \quad , \quad -\infty < y < \infty \quad ,$$
$$y \rightarrow y + 2l \ (\text{periodicity}),\ y \rightarrow -y \ (\text{Z2-parity}) \quad . \qquad (1)$$

Warped Case

$$ds^2 = \frac{1}{\omega^2 z^2}(\eta_{\mu\nu}dx^\mu dx^\nu + dz^2) \quad ,$$
$$-\frac{1}{T} \leq z \leq -\frac{1}{\omega} \text{ or } \frac{1}{\omega} \leq z \leq \frac{1}{T} \ (-l < y < l) \ ,$$
$$z \rightarrow -z \ (\text{Z2-parity}) \quad . \qquad (2)$$

Casimir Energy E_{Cas}

$$\mathrm{e}^{-l^4 E_{Cas}} = \exp\left[-\frac{1}{2} l^4 \int \frac{d^4p}{(2\pi)^4} \{4 \sum_{n \in \mathbf{Z}} \ln(p^2 + {m_n}^2) + \sum_{n \in \mathbf{Z}, n \neq 0} \ln(p^2 + {m_n}^2)\} \right] , \qquad (3)$$

$p^2 \equiv p_\mu p^\mu$, $m_n = \frac{n\pi}{l}$.

The standard way, taken by Appelquist and Chodos '83, gives

$$V(l) = \frac{1}{5} l \Lambda^5 - \frac{3}{4}\frac{\zeta(5)}{l^4} \ , \ F(l) = -\frac{\partial V}{\partial l} = -\frac{1}{5}\Lambda^5 - 3\frac{\zeta(5)}{l^5} \ . \quad (4)$$

2. P/M Propagator

P/M Propagator

$$G_p^{\mp}(y,y') = \frac{1}{2l}\sum_{n\in\mathbf{Z}}\frac{1}{k_n^2+p^2}\frac{1}{2}\{\mathrm{e}^{-ik_n(y-y')} \mp \mathrm{e}^{-ik_n(y+y')}\} \quad , \tag{5}$$

Casimir energy in terms of P/M propagators.

$$E_{Cas}(l) = \int \frac{d^4p}{(2\pi)^4}\int_{p^2}^{\infty}\{2\mathrm{Tr}G_k^{+}(y,y') + \frac{1}{2}\mathrm{Tr}G_k^{-}(y,y')\}dk^2 \tag{6}$$

The P/M propagators $G_k^{\mp}$ can be expressed in a closed form:

$$G_k^{\mp}(y,y') = \pm\frac{\cosh\tilde{k}(|y+y'|-l) \mp \cosh\tilde{k}(|y-y'|-l)}{4\tilde{k}\sinh\tilde{k}l} ,$$

$$\tilde{k} \equiv \sqrt{k_\mu k^\mu} \ , \ k_\mu k^\mu > 0, \text{(space-like)} \ , \tag{7}$$

3. UV and IR Reg. Parameters and Casimir Energy Evaluation

The integral region: See Fig.1
the UV and IR regularization cut-offs: $\mu \leq \tilde{p} \leq \Lambda$, $\epsilon \leq y \leq l$
We take

$$\epsilon = \frac{1}{\Lambda} \quad , \quad \mu = \frac{1}{l} \quad . \tag{8}$$

Figure 1: Space of (y,$\tilde{p}$) for the integration.

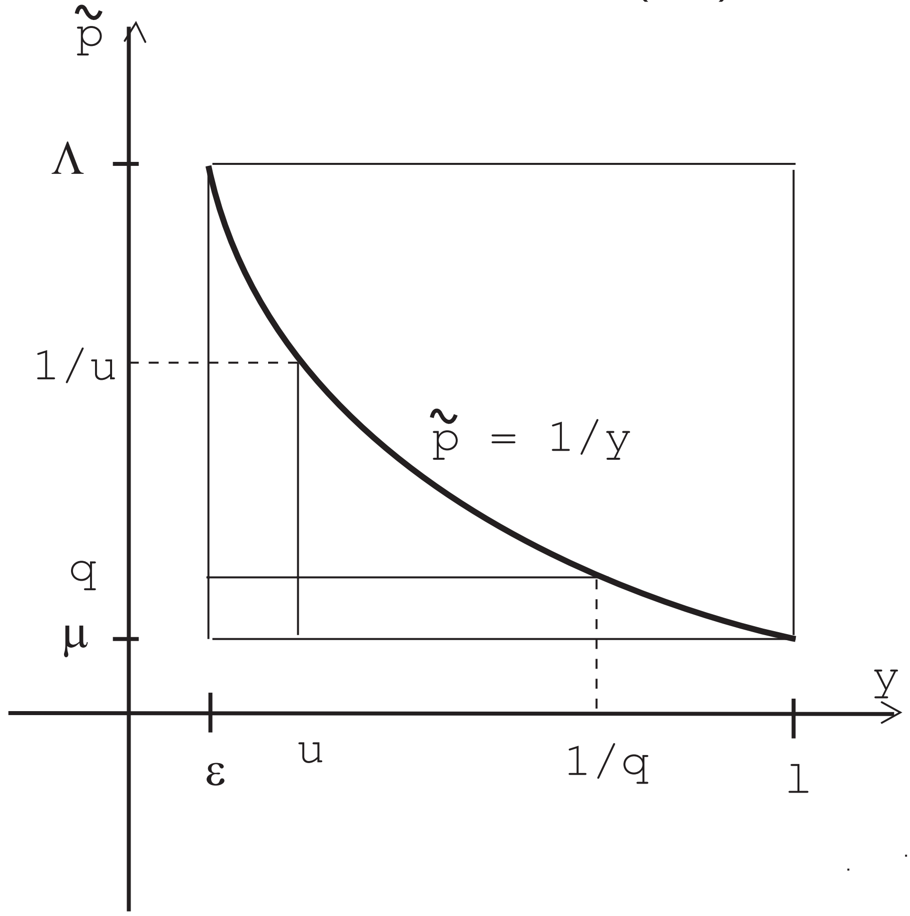

(Λ, l)-*regularized* value of (6).

$$E_{Cas}(\Lambda, l) = \frac{2\pi^2}{(2\pi)^4} \int_{1/l}^{\Lambda} d\tilde{p}\ \tilde{p}^3 \int_{1/\Lambda}^{l} dy F(\tilde{p}, y)\ ,$$

$$F(\tilde{p}, y) = \int_{\tilde{p}}^{\Lambda} d\tilde{k} \frac{-3\cosh\tilde{k}(2y-l) - 5\cosh\tilde{k}l}{2\sinh(\tilde{k}l)}\ . \qquad (9)$$

The integral region: the *rectangle* shown in Fig.1
The integrant of (9),$\tilde{p}^3 F(\tilde{p}, y)$, can be analytically obtained.
Note: the rigorous expression of the regularized quantity.

Figure 2: Behaviour of $\tilde{p}^3 F(\tilde{p}, y)$. $l = 1$, $\Lambda = 10$, $0.1 \leq y < 1$, $1 \leq \tilde{p} \leq 10$.

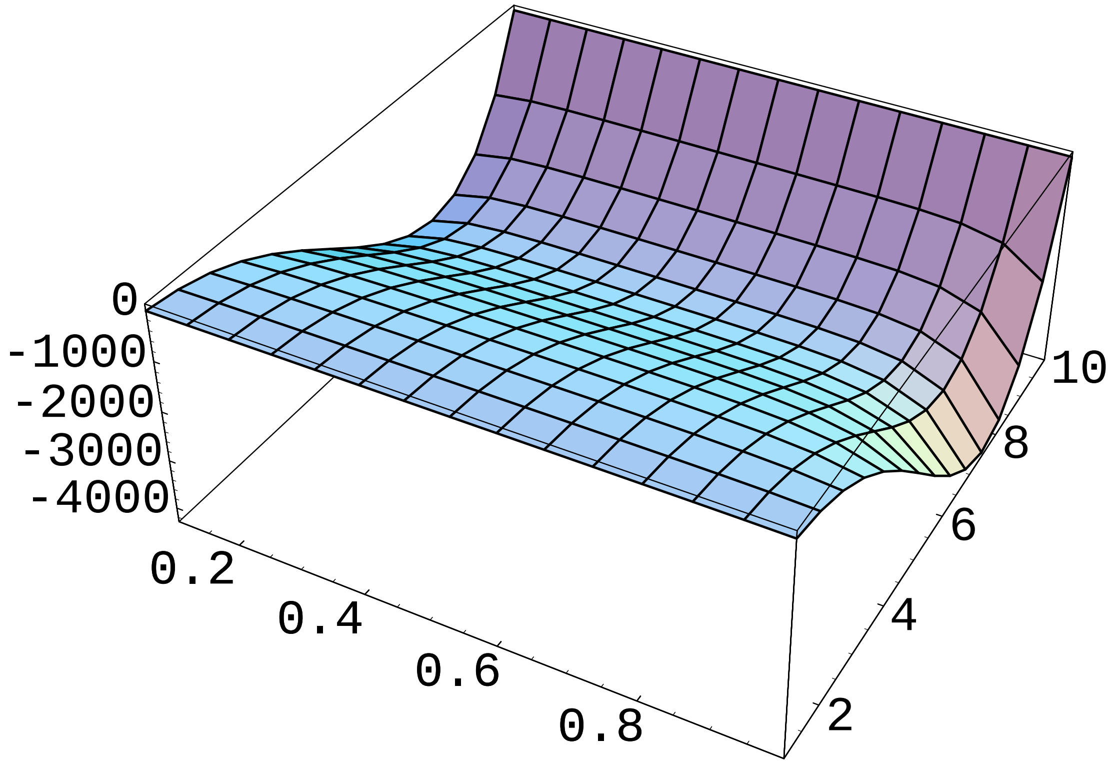

· There is a dip along $\tilde{p}$ axis.
· Flat along y axis.
· The volume of the inside of the shaded surface is E_{Cas}.
· The bottom line of the valley is approximately $\tilde{p} \sim 0.75\Lambda$(constant). $\rightarrow$ $F(\tilde{p}, y) \approx -(f/2)(\Lambda - \tilde{p}),\ f = 5$.
A close numerical analysis of $(\tilde{p}, y)$-integral (9) gives

$$E_{Cas} = \frac{2\pi^2}{(2\pi)^4} \Big[-0.1247 l \Lambda^5 - \frac{1.773 \times (10)^{-16}}{l^4} - 1.253 \times (10)^{-15} \frac{\ln(\Lambda l)}{l^4} \Big] . \qquad (10)$$

Note: $\frac{1}{8} = 0.125$. The leading Λ^5-term, OK.

4. UV and IR Reg. Surfaces and Priciple of Minimal Area

The Λ^5-divergence $\longrightarrow$ How to avoid it ?
legitimately restrict the integral region in $(\tilde{p}, y)$-space

The proposal by Randall and Schwartz '01
the position-dependent cut-off, $\mu < \tilde{p} < 1/u \ , \ u \in [\epsilon, l]$ (See Fig.1)
(They succeeded in obtaining the finite β-function in the 5D warped vector model.)
legitimate?
We propose an alternate(improved?) version of theirs (S.I. & A.Murayama, '07) and give a legitimate explanation within the 5D QFT.

Figure 3: Space of (y,$\tilde{p}$) for the integration (present proposal).

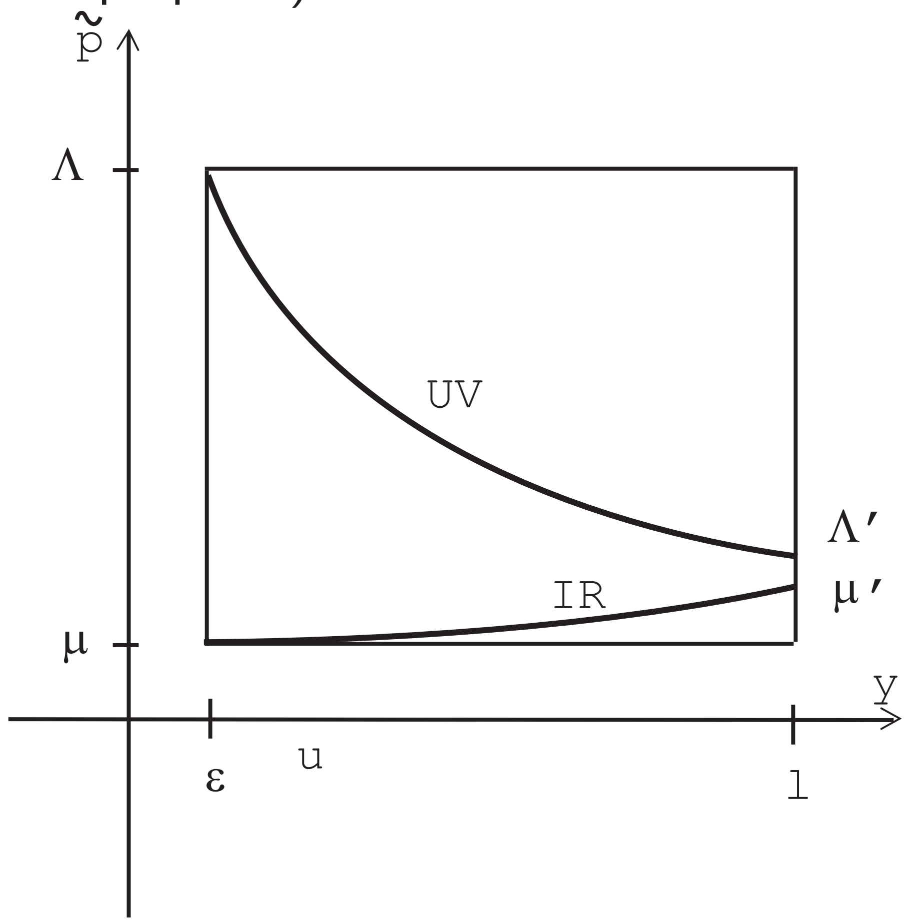

On the "3-brane" at $y = \epsilon$
we introduce the IR-cutoff μ and the UV-cutoff Λ ($\mu \ll \Lambda$). See Fig.3.
This is legitimate: we usually do this procedure in the 4D *renormalizable* thoeries.
On the "3-brane" at $y = l$, we have another set of IR and UV-cutoffs, μ' and Λ'.

We consider the case:
$\mu' \leq \Lambda', \ \mu \sim \mu', \ \Lambda' \ll \Lambda.$
($\longrightarrow$ the renormalization flow.)
We claim here, as for the "3-brane" located at each point y ($\epsilon < y < l$), the regularization parameters are determined by

the minimal area principle.
Explanation in the 5D coordinate space (x^μ, y). See Fig.4.

Figure 4: Regularization Surface B_{IR} and B_{UV} in the 5D coorinate space (x^μ, y) and Flow of Coarse Graining (Renormalization).

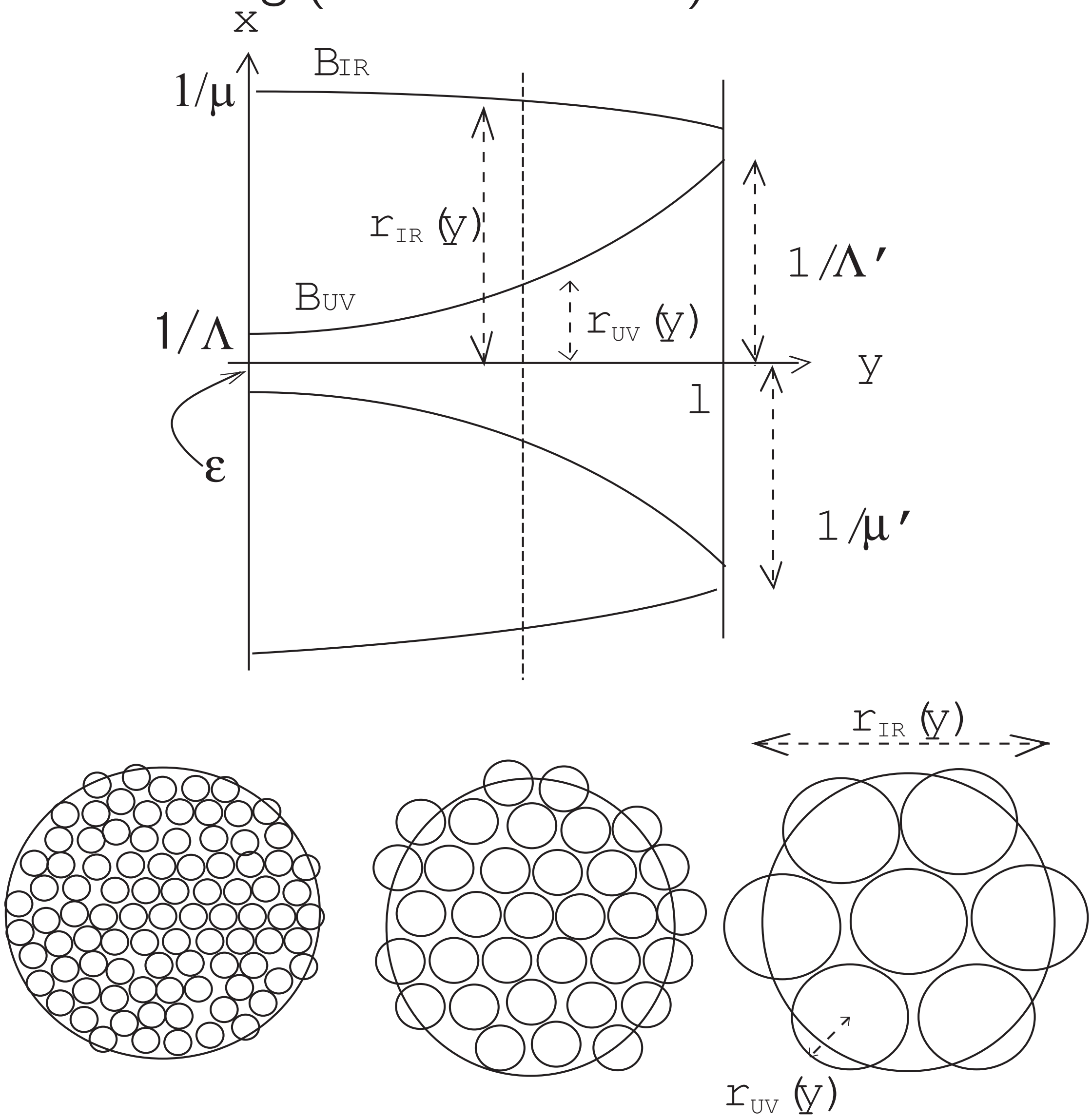

The UV and IR cutoffs change their values along y-axis
Their trajectories make surfaces in the 5D bulk space
We *require* the two surfaces do not cross for the purpose of the renormalization group interpretation. We call them UV and IR regularization surfaces(B_{UV}, B_{IR}). The cross sections

of the regularization surfaces at y: the spheres S^3 with the radii $r_{UV}(y)$ and $r_{IR}(y)$. (Euclidean space for simplicity.)
The UV-surface is shown in Fig.5.

Figure 5: UV regularization surface in 5D coordinate space. This is the *closed string* configuration.

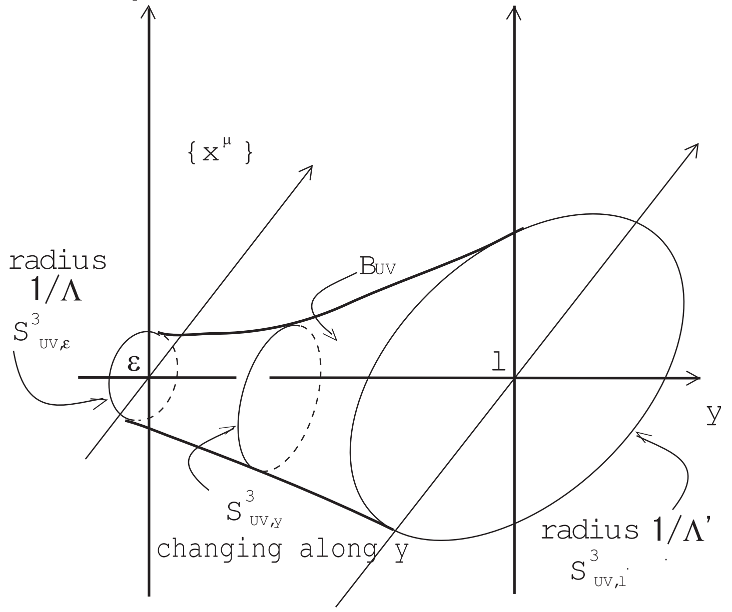

The 5D volume region bounded by B_{UV} and B_{IR} = the integral region of the Casimir energy E_{Cas}.
The forms of $r_{UV}(y)$ and $r_{IR}(y)$ can be determined by the minimal area principle.

$$\delta(\text{Surface Area}) = 0 \ , \ 3 - \frac{r\frac{d^2r}{dy^2}}{1+(\frac{dr}{dy})^2} = 0 \ , \ 0 \leq y \leq l. \quad (11)$$

Two result curves of (11) in Fig.6,7.

Figure 6: Numerical solution of (11). Vertical axis: r; Horizontal axis $0 \leq y \leq l = 1$. IR-curve (upper): $r[0] = 12.0, r'[0] = -1.0$; UV-curve (lower): $r[1.0] = 10.0, r'[1.0] = 350.0$.

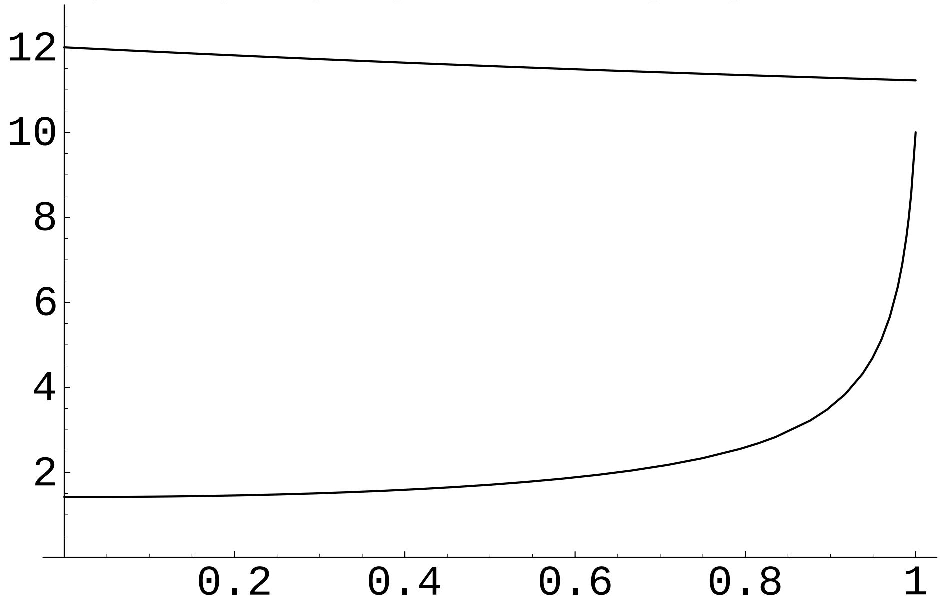

Figure 7: Numerical solution of (11). Vertical axis: r; Horizontal axis $0 \leq y \leq l = 1$. IR-curve (upper): $r[0] = 4.6, r'[0] = -1.0$; UV-curve (lower): $r[0] = 4.5, r'[0] = -22.0$.

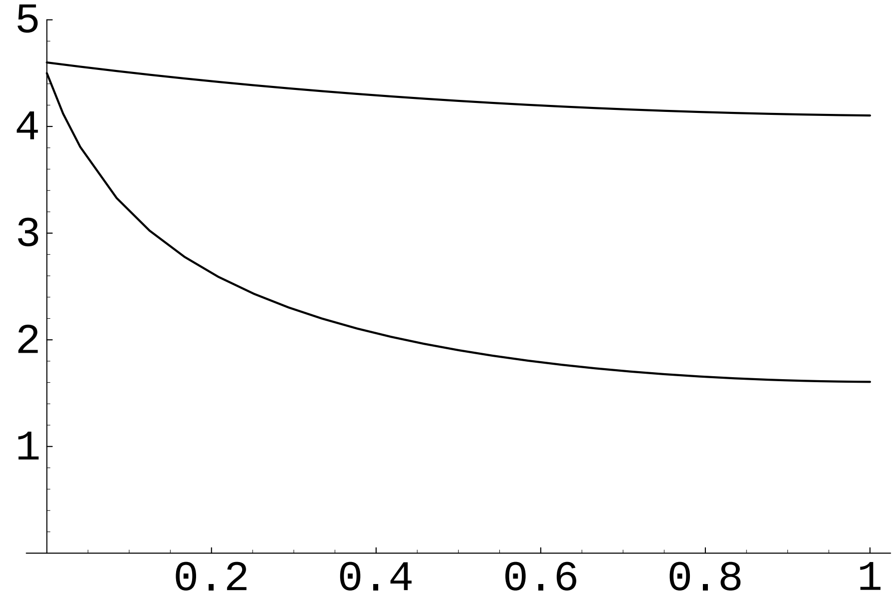

Fig.6 : Fine $\longrightarrow$ Coarse as z Increases
Fig.7 : Coarse $\longrightarrow$ Fine as z Increases

The present regularization scheme also gives the *renormalization group* interpretation to the change of physical quantities along the extra axis. See Fig.4. **Sphere Lattice**

5. Weight Function

We introduce a *weight function* $W(\tilde{p}, y)$ (to suppress UV and IR divergences).

$$E^W_{Cas}(l) \equiv \int \frac{d^4p}{(2\pi)^4} \int_0^l dy \; W(\tilde{p}, y) F(\tilde{p}, y) \quad ,$$

Trial Examples of $W(\tilde{p}, y)$:

$$\left\{ \begin{array}{c} \mathrm{e}^{-\frac{1}{2}l^2\tilde{p}^2-\frac{1}{2}(y^2/l^2)} \equiv W_1(\tilde{p}, y), \ \text{elliptic} \\ \mathrm{e}^{-\frac{1}{2}\tilde{p}^2y^2} \equiv W_3(\tilde{p}, y), \ \text{hyperbolic, R-S type} \\ \mathrm{e}^{-\frac{1}{2}l^2(\tilde{p}^2+1/y^2)} \equiv W_8(\tilde{p}, y), \ \text{reciprocal} \end{array} \right. \qquad (12)$$

Numerical result 1. Flat Case:

$$E^W_{Cas} \times (\frac{1}{\Lambda l}) \times 8\pi^2 =$$

$$\left\{ \begin{array}{lll} \frac{-21.4}{l^4}\left[1-(0.258, 0.130, 0.0650)\cdot 10^{-3}\ln\Lambda\right] & \text{for} & W_1(\tilde{p}, y) \\ -0.270\frac{\Lambda^3}{l}\left[1-(21.9, 10.9, 5.44)\cdot 10^{-5}\ln\Lambda\right] & \text{for} & W_3(\tilde{p}, y) \\ \frac{-1.00}{l^4}\left[1-(4.04, 2.02, 1.01)\cdot 10^{-4}\ln\Lambda\right] & \text{for} & W_8(\tilde{p}, y) \end{array} \right.$$

Numerical result 2. Warped Case:

$$E^W_{Cas} \times (\frac{T}{\Lambda}) \times 4\pi^2 =$$

$$\left\{ \begin{array}{ccc} -0.336\omega^4\left[1+3.15\cdot 10^{-2}\ln\Lambda\right] & \text{for} & W_1(\tilde{p},z) \\ -2.62\cdot 10^{-2}\omega\Lambda^3\left[1-4.85\cdot 10^{-5}\ln\Lambda\right] & \text{for} & W_3(\tilde{p},z) \\ -0.104\omega^4\left[1+2.56\cdot 10^{-2}\ln\Lambda\right] & \text{for} & W_8(\tilde{p},z) \end{array} \right. \quad (14)$$

The (UV) divergences much reduces compared with the un-weighted case $W(\tilde{p},y)=1$ of Λ^5.
W_3: Randall-Schwartz's proposal.

Renormalization of ω

$$E^W_{Cas}/\Lambda T^{-1} = -\alpha\omega^4\left(1-4c\ln(\Lambda/\omega)\right) = -\alpha\omega'^4 \quad , \\ \omega' = \omega\sqrt[4]{1-4c\ln(\Lambda/\omega)} \quad . \quad (15)$$

$$|c| \ll 1 \quad , \quad \omega' = \omega(1-c\ln(\Lambda/\omega)) \quad , \\ \beta_\omega = \frac{\partial}{\partial(\ln\Lambda)}\ln\frac{\omega'}{\omega} = -c \quad . \quad (16)$$

Figure 8: Behavior of $-\ln|E_{Cas}|$ for Flat case , weight W_1 and $l = 40$. $\Lambda = 10 \times (1, 2, 4, 8, 16, 32, 64, 128)$.

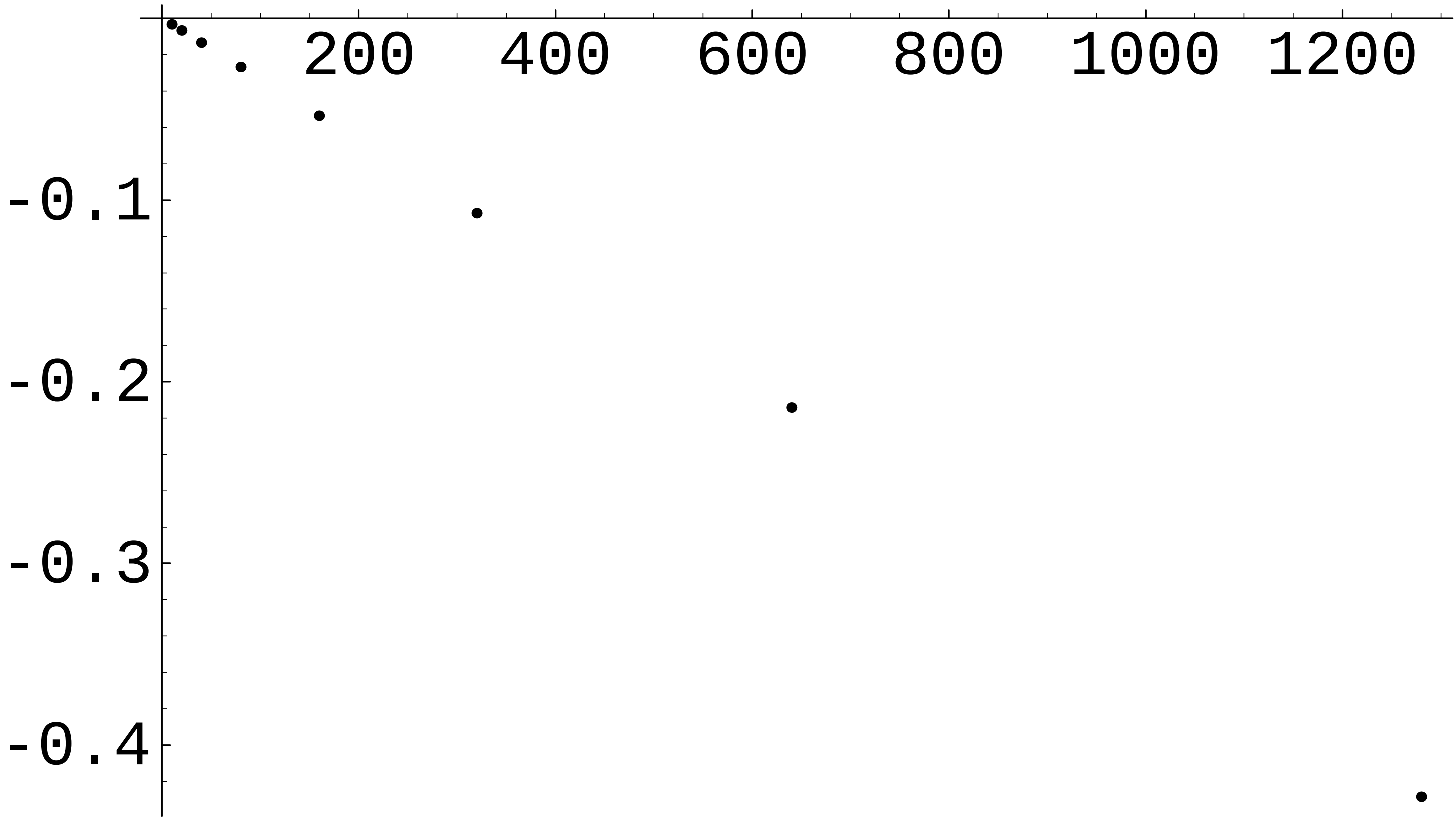

Figure 9: Behavior of $-\ln|E_{Cas}|$ for Warped case , weight W_8, $T = 0.1$ and $\omega = 1000$. $\Lambda = 10^4 \times (1, 2, 4, 8, 16)$.

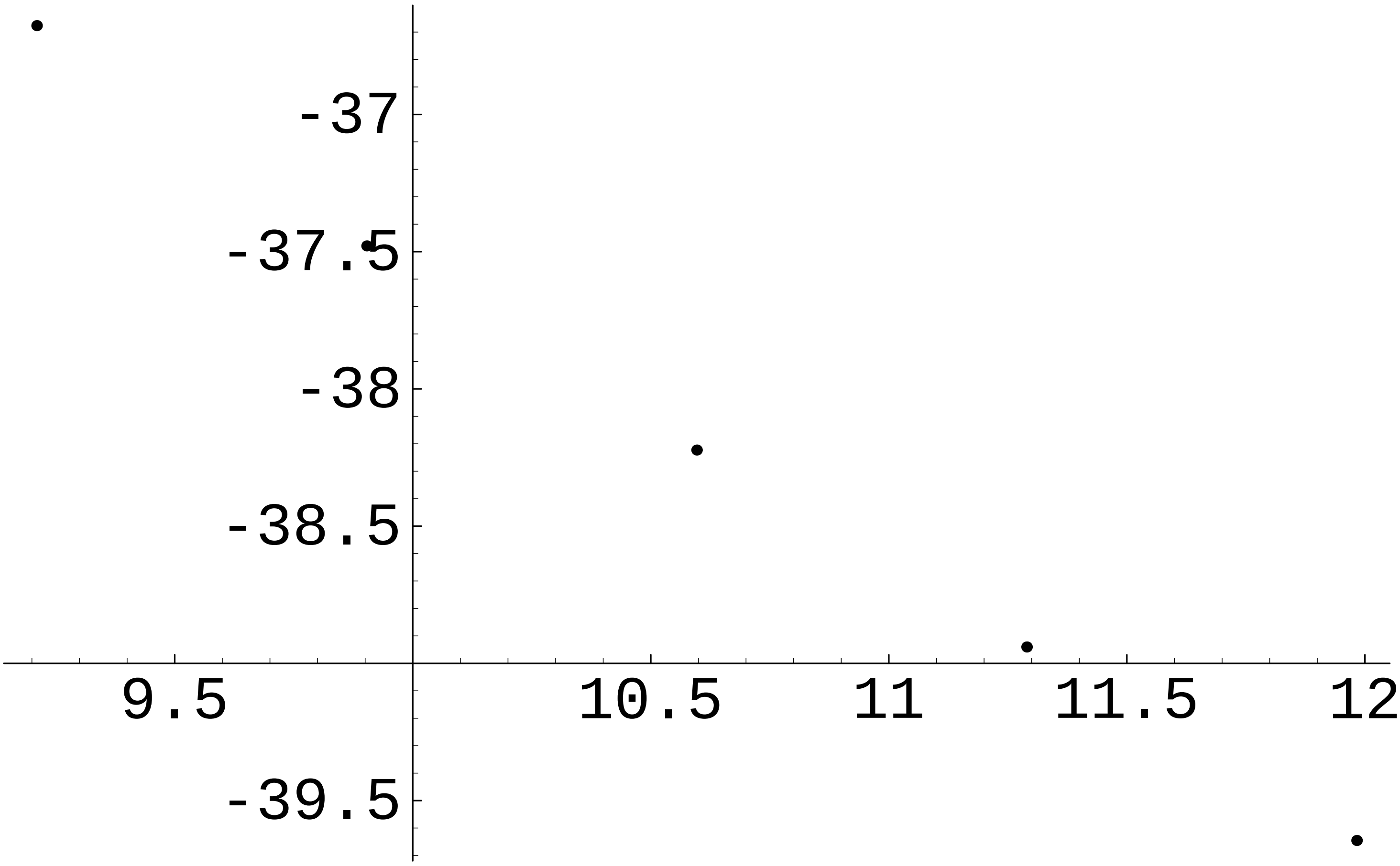

6. Meaning of Weight Function $W(\tilde{p}, y)$

The Casimir energy is reexpressed as

$$E^W_{Cas}(l) = \int d^4x \int_0^l dy\ \hat{W}(r(x), y)\hat{F}(r(x), y) \quad . \qquad (17)$$

The dominant contribution to E_{Cas}, $r_W(y)$, is given by the minimal principle of the "action",(17). We require $r_W(y)$ coincides with the geodesic $r_G(y)$ which is determined by the *minimal area principle* (11).

Figure 10: Behaviour of $\tilde{p}^3 W_6(\tilde{p}, y) F(\tilde{p}, y)$(parabolic suppression2). $\Lambda = 10, \ l = 0.5$. $1.001/\Lambda \leq y \leq 0.99999 l, \ 1/l \leq \tilde{p} \leq \Lambda$. The contour of this graph is given later in Fig.11.

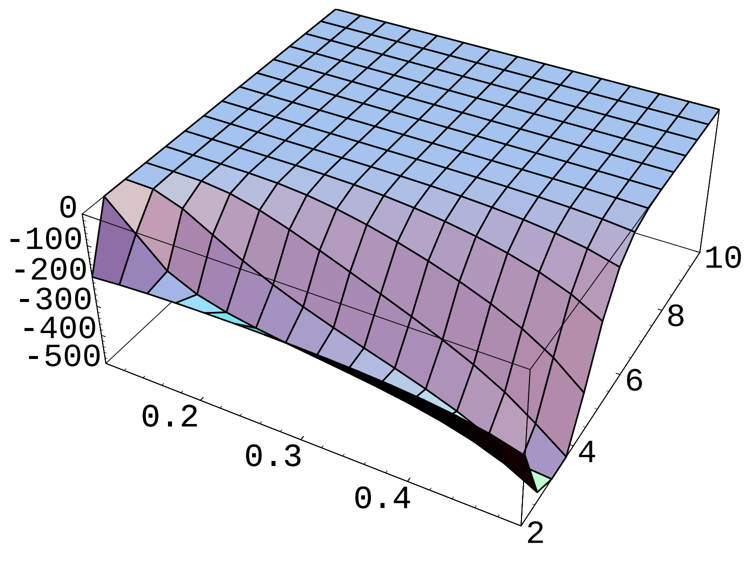

Figure 11: Contour of $\tilde{p}^3 W_6(\tilde{p}, y) F(\tilde{p}, y)$(parabolic suppression2, Fig.10). $\Lambda = 10, \ l = 0.5$. Horizontal axis: $1.001/\Lambda \leq y \leq 0.99999l$, Vertical Axis: $1/l \leq \tilde{p} \leq \Lambda$.

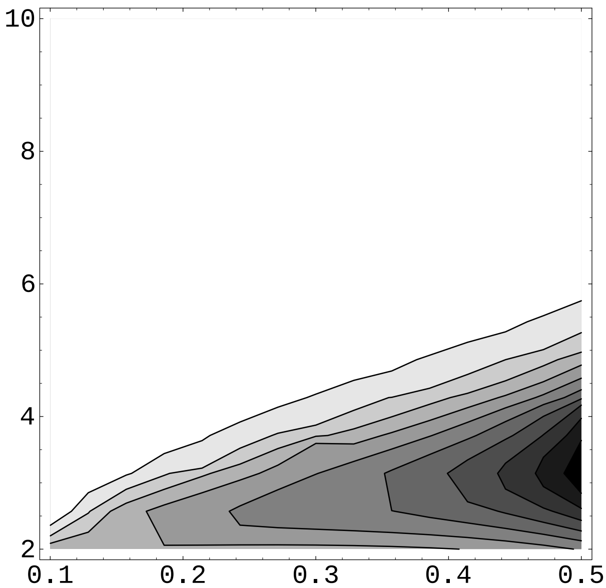

Figure 12: Geodesic Curve $1/r_-(y), C = 5.1215, C' = 1.068$ in (**??**). Horizontal axis: $0 \leq y \leq 0.5$, Vertical Axis: $0 \leq 1/r_- \leq 3$.

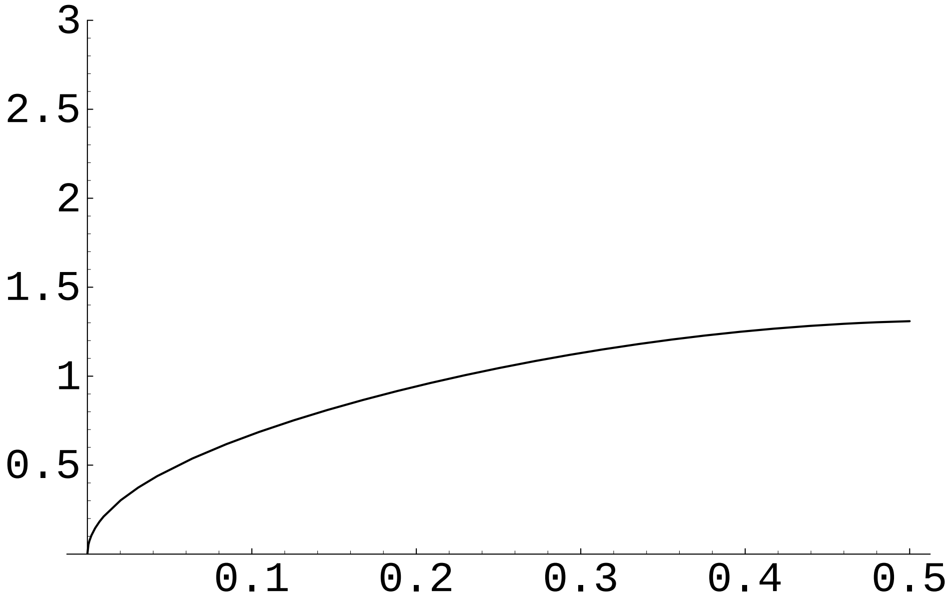

Figure 13: Behaviour of $(-1/2)\tilde{p}^3 W_4(\tilde{p},z)F^-(\tilde{p},z)$(linear suppression). $\Lambda = 100$, $\omega = 10$, $T = 1$. $1.0001/\omega \le z \le 0.9999/T,\ \mu = \Lambda T/\omega \le \tilde{p} \le 25.$

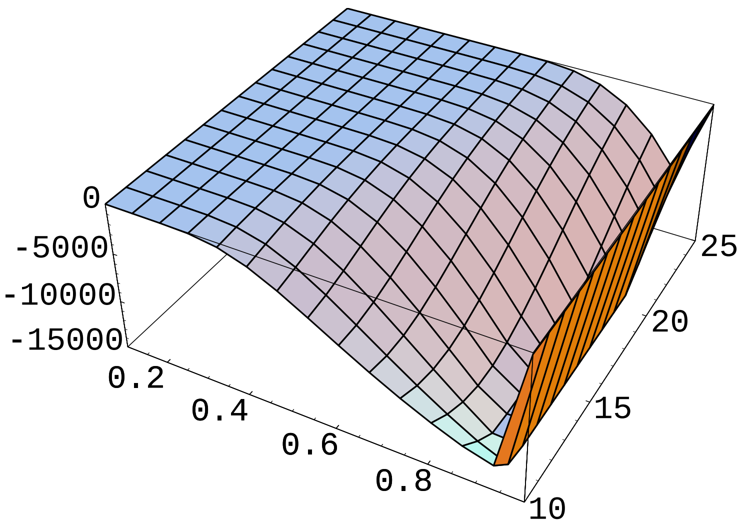

Figure 14: Contour of $(-1/2)\tilde{p}^3 W_4(\tilde{p},z)F^-(\tilde{p},z)$(linear suppression, Fig.13). $\Lambda = 100$, $\omega = 10$, $T = 1$. $1.0001/\omega \le z \le 0.9999/T,\ \mu = \Lambda T/\omega \le \tilde{p} \le 25.$

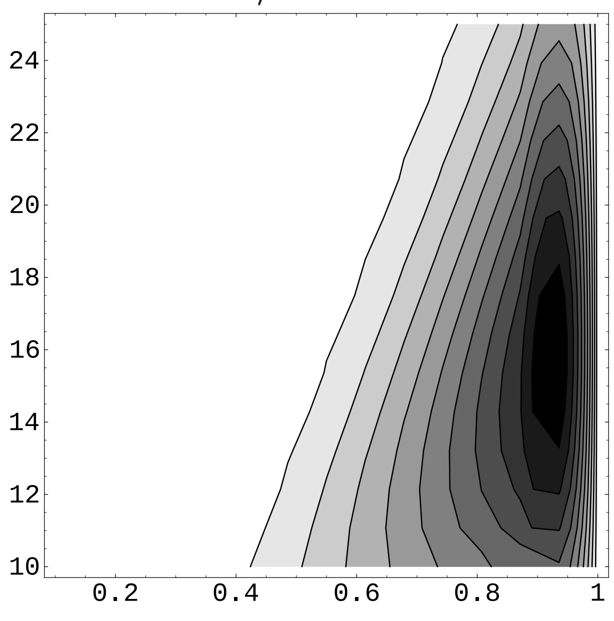

Figure 15: Geodesic Curve $\tilde{p}(z)$. $\tilde{p}(1.0) = 30.0$, $\tilde{p}'(1.0) = 10.0$. Horizontal axis: 0.0001$\leq$ z $\leq$ 1.0 ; Vertical axis: $0.0 \leq \tilde{p} \leq 30.$

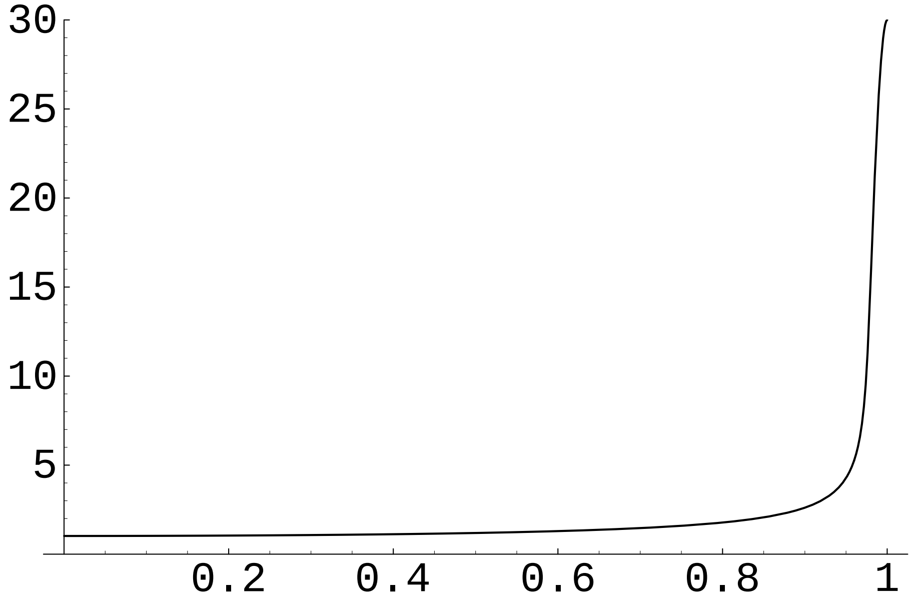

We *newly define* the Casimir energy in the higher-dimensional theory as follows.

$$\mathcal{E}_{Cas}(\omega, T) \equiv \int_{1/\Lambda}^{1/\mu} d\rho \int_{r(1/\omega)=r(1/T)=\rho} \prod_{a,z} \mathcal{D}x^a(z) F(\frac{1}{r}, z)$$

$$\times \exp\left[-\int_{1/\omega}^{1/T} \frac{1}{\omega^4 z^4} \sqrt{r'^2 + 1}\ r^3 dz \right] \quad ,(18)$$

where $\mu = \Lambda T/\omega$ and the limit $\Lambda \to \infty$ is taken.

7. Conclusion

We have analyzed 5D quantum electro-magnetism in the recent standpoint. To make the theory finite, we have proposed a new regularization procedure based on the minimal area principle. Casimir energy is finitely obtained.

- formulation in terms of the heat-kernel
- Casimir energy is expressed in a closed form
- UV and IR regularization surfaces and minimal area principle.
- Numerical evaluation of Casimir energy and the bulk geodesic curve (11).
- Sphere lattice structure and renormalization flow, the β function

We hope the present analysis advances further development of the higher dimensional field theory.